Ultrasonics 94 (2019) 350–363

Contents lists available at ScienceDirect

Ultrasonics

journal homepage: www.elsevier.com/locate/ultras

Machining forces in ultrasonic-vibration assisted end milling

Girish Chandra Verma[a], Pulak Mohan Pandey[a,*]

[a] Department of Mechanical Engineering, Indian Institute of Technology Delhi, Delhi 110016, India

ARTICLE INFO

Keywords:
Ultrasonic assisted milling
Axial vibration
Milling forces
Standard deviation in milling forces
ANOVA

ABSTRACT

Ultrasonic assisted milling (UAM) is one of the advancements in the area of conventional milling process. Literature suggests that superpositioning of ultrasonic vibration with milling process improves its efficacy by reducing forces and improving surface finish. In the present study experimental investigations were carried out to evaluate the effect of process parameters (power of ultrasonic vibration (UP), rotational speed, axial depth of cut (DOC) and feed rate) on the cutting responses (average cutting force and the standard deviation in cutting forces). An experimental setup was designed and developed to perform UAM process with axial vibrations. The end mill used in this setup was designed by performing harmonic analysis on ANSYS workbench. UAM experiments based on central composite design (CCD) technique were performed on Al6063 aluminum alloy. Analysis of variance (ANOVA) was performed and regression equations were obtained. Further, the obtained results were analyzed to study the effect of machining parameters on the responses. The developed models were then validated by performing experiments on random and optimized set of process parameters. The ANOVA results suggested that the most effective parameter for cutting forces was feed rate, however its standard deviation was affected by rotational speed. Also the assistance of axial vibration reduced the average cutting force and increased its standard deviation. In order to evaluate the effect of axial ultrasonic vibrations, simulations were performed to study the cutting kinematics in UAM process. The simulations showed that the presence of torsional vibration at the cutting tip, caused intermittent cutting during UAM.

1. Introduction

At present milling is one of the most common manufacturing processes in industries as it can produce complex components like thin walled structure, freeform surfaces etc. However, milling of newly developed materials like high-strength aerospace alloys causes high cutting forces, rapid wear of cutting edges, and poor surface roughness [1]. Occurrence of these problems causes tool deflection and results in inaccurate products. In order to avoid the problems associated with the milling of hard materials some advancements were made in the process. Application of coolant is the most commonly used technique to cater the above problem. However the use of coolant makes machining costly and ecologically harmful [2]. Growing demands for machining of these materials require improvement in the milling process.

A few techniques were developed to avoid the problems associated with the milling of hard materials. The most commonly used technique among them is high speed milling which causes reduction in the cutting forces [3]. However at high speed milling occurrence of chatter becomes very prominent [4] which results in rapid tool wear and low surface quality [1]. In order to avoid chattering, Liu et al. [5] have analytically modeled it by considering system responses and cutting forces. Using these studies, the chatter stability lobes were plotted which provided the parameters for chatter free milling.

Minimum quantity lubrication (MQL) has been tried in milling, to minimize the problems associated with machining of hard materials. In MQL, a small amount of lubrication is applied to the cutting zone which causes lowering in cutting force and improvement of surface finish. Researchers [6,7] have also tried MQL with nano particles and found that cutting forces and surface roughness further reduced. The experimental studies [8,9] showed that formation of a thin film in the secondary shear zone resulted in lowering of frictional coefficient.

Milling with ultrasonic vibration assistance is one of the methods to machine hard materials. Several researchers [10–13] have reported that the assistance of ultrasonic vibration in milling operation resulted in reduced cutting forces and surface roughness. In late 1960s, the ultrasonic vibration was first applied to the macro scale turning operation, which resulted in lower cutting forces [14]. Several attempts [15] were made to evaluate the effect of ultrasonic vibration assistance in different manufacturing processes like UAM (ultrasonic assisted milling), UAD (ultrasonic assisted drilling) etc. Researchers [11,16,17] have suggested that the reduction in cutting force is mainly due to intermittent cutting. The phenomenon of intermittent cutting occurs due to

* Corresponding author.
E-mail address: pmpandey@mech.iitd.ac.in (P.M. Pandey).

https://doi.org/10.1016/j.ultras.2018.07.004
Received 27 June 2017; Received in revised form 12 June 2018; Accepted 11 July 2018
Available online 18 July 2018
0041-624X/

superposition of to and fro motion during conventional cutting operation. This motion generates an additional velocity V_{ul} (velocity of cutting edge due to ultrasonic vibration) at the cutting tip. Additionally, the intermittent cutting only occurs when V_{ul} becomes higher than the cutting velocity [15].

Nath and Rahman [18] modeled the intermittent cutting effect in turning by calculating tool and workpiece contact ratio (contact ratio is the ratio of time of contact in one oscillation to time period of oscillation) during ultrasonic assisted turning (UAT) experiments. They have proposed that the average force during ultrasonic assisted cutting is the same as contact ratio multiplied by the normal cutting force. They have validated the proposed model by performing comparative UAT experiments on Inconel 718.

Several studies [10–13,16,19–28] were performed to understand the UAM process. Experimental studies [19,21,23,27,28] have showed that the application of axial ultrasonic vibration results reduction in cutting forces, surface roughness, cutting temperature and tool wear. Important attempts in the direction of UAM are summarized as under.

Maurotto and Wickramarachchi [24] analyzed the effect of vibration frequency (axial vibration) in ultrasonic assisted end-milling (carbide) of AISI 316l. Their experimental results showed that with the increase in vibration frequency surface roughness the increases. They also found that frequency of 40 kHz is the most unsuitable for the UAM as tool wear and residual stresses were found to be maximum. However, performing UAM at 20 kHz resulted in enhanced tool life as compared to UAM at other frequencies (40 kHz and 60 kHz).

Shen et al. [16] experimentally analyzed the effect of ultrasonic vibrations on slot milling operation. They compared the effect of ultrasonic vibration assistance in milling operation by measuring cutting forces, surface roughness, chip morphology and slot dimensional accuracy. They concluded that ultrasonic vibration aids the milling operation by performing pulse-like cutting operation. Zarchi et al. [10] measured the cutting forces in side milling of X20Cr13 stainless steel with the assistance of ultrasonic vibrations (in feed rate direction). They also analyzed the effect of process parameters on cutting forces during ultrasonic assisted side milling. Their experimental results showed 42% reduction in cutting forces due to intermittent cutting. It was found that as the cutting speed increased, the ultrasonic effect decreased and the UAM process transformed into conventional milling process.

Li and Wang [20] studied the effect of process parameter on tool wear and surface roughness in UAM of SKD61 Tool Steel. Their experimental results showed that the assistance of axial ultrasonic vibration improves the milling process by reducing tool wear, surface roughness and burr height. The results also show that effect of ultrasonic vibration decreases with increase in rotational speed.

Elhami et al. [25] studied the effect of machining parameters on cutting forces during ultrasonic assisted milling of thermally enhanced hardened AISI 4140. They have also proposed an analytical model for the same by considering the effect of vibration on instantaneous chip thickness. Their model also included a 3D heat transfer model to predict the temperature field in the workpiece in order to incorporate the effect of thermal enhancement on cutting forces.

Wang et al. [29] studied the kinematics of the milling tool with superimposed vibration. Their simulation results showed that due to the presence of ultrasonic vibrations, the helical milling tool executed vibrations simultaneously (a) axial and (b) torsional vibrations. This vibration superimposes an additional ultrasonic velocity V_{ul} (Eq. (9) at the cutting tip and increases with increase in ultrasonic power.

Zarchi et al. [11] proposed an analytical model to predict the cutting forces in ultrasonic assisted milling. They considered change in the un-deformed chip thickness which occurred due to ultrasonic vibrations provided to the workpiece. Developed model was then validated by performing experiments on AISI 420 stainless steel. Shen et al. [17] developed an analytical model by considering the effect of vibration on instantaneous chip thickness. Their results were validated by performing slot milling with the assistance of ultrasonic vibration on aluminum (Al6061).

Ding et al. [13] developed a model to predict three-dimensional cutting forces in two-dimensional vibration-assisted micro milling (2-D VAMM). Instantaneous chip thickness was evaluated by considering the machine dynamics in cutting force model. The experimental results showed that consideration of machine dynamics led to more accurate prediction of cutting forces.

Verma et al. [30] developed a model to predict three-dimensional cutting forces in axial ultrasonic vibration-assisted milling. In the model effect of acoustic softening and intermittent cutting with milling model were integrated for the prediction of UAM forces. The results showed that the present model predicts the UAM forces within ± 15% of deviation at the meso scale for Al6063 alloy.

As it can be seen from the literature review, there has been no study which evaluates the effect of process parameters in UAM process with axial vibration. The present work intends to fill the above mentioned research gap by conducting experimental investigations for UAM process. Thus, an experimental setup was designed by performing harmonic analysis on ANSYS workbench software. Furthermore, process parameters with their effective ranges were chosen for designing the experiments. Experiments based on central composite designing methodology were performed on Al6063 aluminum alloy, to develop a statistical model for cutting forces and their standard deviation. Further, the developed model was verified by performing confirmation experiments at intermediate and optimized set of process parameters. He results were then analyzed from the main effect plots and interaction graphs, for all the effective parameters. In order to evaluate the effect of axial ultrasonic vibration on cutting kinematics, simulation was performed for the developed UAM tool. The simulation results showed the presence of ultrasonic vibration at the cutting tip which results in intermittent cutting.

2. Design and fabrication of tool

In order to perform the UAM with axial vibration an experimental setup was designed and fabricated as shown in Fig. 1. The setup consists of an ultrasonic assisted milling assembly which can be mounted on the head of CNC milling machine. The assembly has three major components which are presented in Table 1.

The end milling tool (specification of the tool is given in Table 2) used in the assembly was specifically designed for the UAM process, as it acts as a part of the horn.

Brass was used to provide rigidity to the horn and Metalon provided electric insulation between the horn and collet. Copper rings provided on the collar were utilized for supplying power to piezoelectric crystal. The schematic diagram and actual picture of the designed and fabricated assembly to perform ultrasonic assisted milling has been presented in Fig. 1.

The 3D CAD model of the horn and the tool were built and assembled on Solidworks 14, further it was used for the FEM analysis in ANSYS Workbench 14.5. Additionally, modal and harmonic analysis were performed to evaluate the natural frequencies, amplification factor and stress concentration in the horn during vibration. Simulation results (Fig. 2a) show that the horn has high amplification factor (~5) at 20.0 kHz. In addition, the stress concentration (~74 MPa) (Fig. 2b) in the horn was less than yield stress value (~210 MPa) of the material. Hence, there will be no permanent deformation in the assembly during the ultrasonic vibration. All these simulation results show that the designed horn assembly can be used to perform UAM experiments.

A power supply of 800 W with 20 kHz frequency was given to the assembly through the carbon brushes. The voltage of power supply can be varied to achieve different amplitudes at the tool tip. The maximum amplitude of ~20 μm was measured at the tip of the tool by using dial gauge (with least count of 1 μm). The frequency of vibration at the tool tip was also verified using accelerometer.

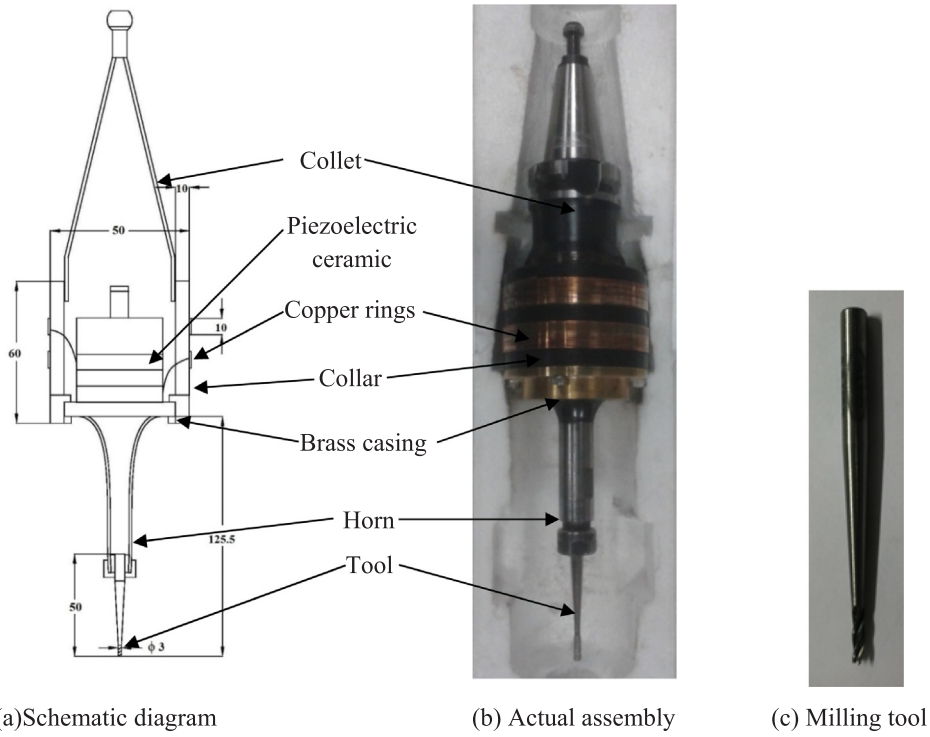

(a)Schematic diagram (b) Actual assembly (c) Milling tool

Fig. 1. Ultrasonic assisted milling assembly.

Table 1
Description of various components of ultrasonic assisted milling assembly.

Component	Material	Purpose
Collar	Metalon	Acts as an attachment between casing and collet
Casing	Brass	Acts as an attachment between collar and tool
Tool	HSS	Acts as a part of the horn and performs cutting
Horn assembly	AISI 316	Generates and transmits vibration to the tool through horn

Table 2
Specification of the tool used in the experiments.

Tool material	Diameter (mm)	No. of flute	Helix angle	Rake angle	Clearance angle
HSS	3	4	30°	10°	5°

3. Ultrasonic assisted milling experiments

The experimental setup (Fig. 3) for measuring the cutting forces in UAM, consisted of the designed UAM assembly, 3 axis vertical CNC milling machine and a dynamometer. UAM assembly was mounted on the head of CNC milling machine (HyTech CNC machine) with carbon brush arrangement. The dynamometer (Schunk Delta SI30-30) was rigidly mounted on the bed with the required fixture to hold the workpiece. Fig. 3 shows the designed experimental setup for UAM experiments. Workpiece of Al6063 alloy of size 30 × 30 × 10 mm^3 were used for all the experiments. These workpieces were prepared from the same lot to avoid any error due to the difference in material properties. In addition, the experiments were performed in the same ambience with a fresh tool to minimize the error.

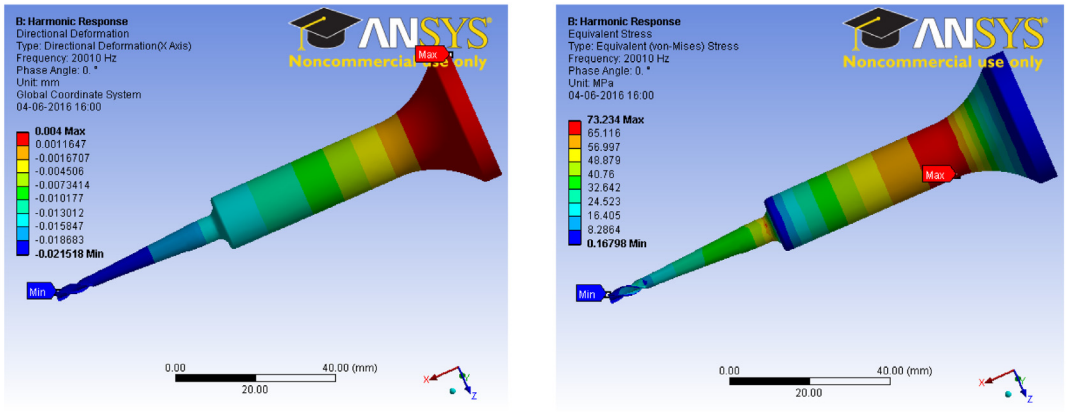

Deformation analysis Stress analysis

Fig. 2. FEM analysis of tool and horn assembly.

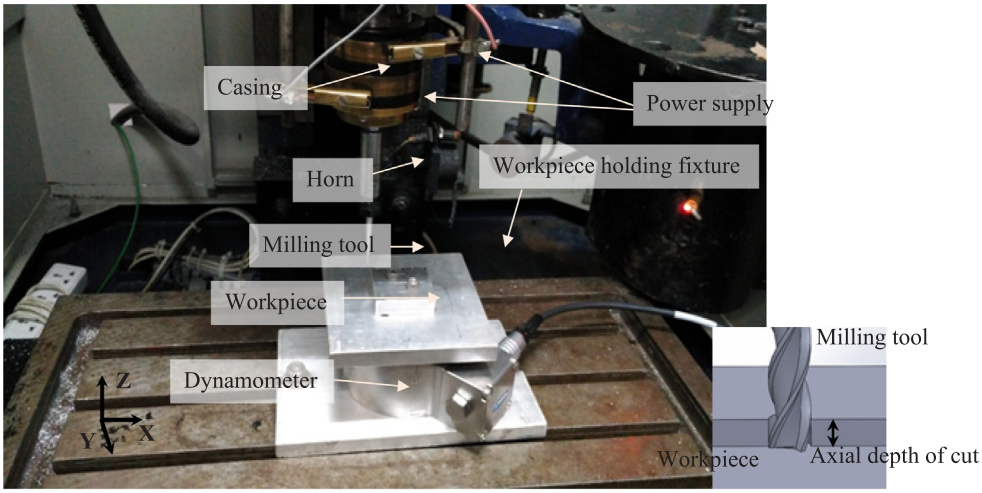

Fig. 3. Experimental setup.

3.1. Process parameters

As milling is an intermittent cutting process, the cutting forces vary with time and follow a sinusoidal pattern. This is due to the sinusoidal variation in the chip thickness during the process and this variation is different for up milling, down milling and slot milling. Researchers [31,32] have considered the mean and standard deviation in the cutting forces separately to study the milling process. However, in UAM the variation is very rapid due to the presence of vibration during cutting. The pilot UAM experiments have shown that mean as well as the deviation in cutting force change with the machining parameters. Therefore, the present study evaluates the effect of process parameters on the mean UAM forces (F_X, F_Y and F_Z) and their standard deviations ($\sigma(F_X)$, $\sigma(F_Y)$ and $\sigma(F_Z)$).

In order to study the UAM process, four process parameters were selected, based on literature [10,11,16,17]. The range of the process parameters used in the experiments was based on machine limitations and the results of pilot experiments. The result of the pilot experiments showed that as the rotational speed increased the effect of axial ultrasonic vibration (at low ultrasonic power) diminished. Hence, to evaluate the effect of ultrasonic power, the upper limit of the rotational speed was kept at 2625 RPM. Upper limit of feed rate and axial depth of cut was fixed to avoid chattering effect during UAM. For designing the experiments, CCD methodology was considered because it yields quadratic and interaction effect of process variables on the response by performing lesser number of experiments [33].

$$Y = \beta_o + \sum_{i=1}^{n} \beta_i X_i + \sum_{i=1}^{n} \beta_{ii} X_i^2 + \sum_{i=1}^{n} \sum_{j>i}^{n} \beta_{ij} X_i X_j + \varepsilon$$

where Y is the response variable; n is the number of variables; β_i, β_{ii} and β_{ij} are the constants; ε is the random error; and X_i, X_i^2 and X_iX_j are the first-order, second-order, and the interaction terms of the process factors, respectively. Table 3 shows the process factors with their levels, which were used for the DOE.

Table 3
Parameters with their levels chosen for experiments.

Factors		Levels				
X_1	Rotational speed (RPM)	1125	1500	1875	2250	2625
X_2	Ultrasonic power percentage (UP) (%)	20	40	60	80	100
X_3	Axial depth of cut (mm)	0.2	0.4	0.6	0.8	1
X_4	Feed rate (mm/min)	10	30	50	70	90

3.2. UAM experiments

Slot milling experiments were performed using the designed experimental setup. The axis of dynamometer was aligned with the machine axis to accurately measure the components of the cutting forces. All these experiments were performed with clockwise rotating tool and cutting feed rate in Y (–) direction. A sampling frequency of 40 kHz was used to capture the cutting force signals in DAQ, so that frequencies below 20 kHz can be accurately measured (as per Nyquist limit) [34]. Further the UAM forces obtained in the time domain were transformed to frequency domain by Fast Fourier Transform (FFT) as shown in Fig. 4. The FFT results (Fig. 4) shows the presence of ~20 kHz vibration in the cutting forces. However, a small peak at 0.1 kHz shows the effect of tool rotational speed.

Cutting forces in X, Y and Z directions were recorded; further mean and standard deviations were calculated. Table 4 shows the mean cutting forces and standard deviations measured during UAM of Al6063.

4. Statistical analysis

In order to analyze the effect of process parameters, the ANOVA was performed for the above experimental data (Table 4). Further, the regression model was developed for all the responses. Adequacy of the developed models were verified (at 95% confidence level) by

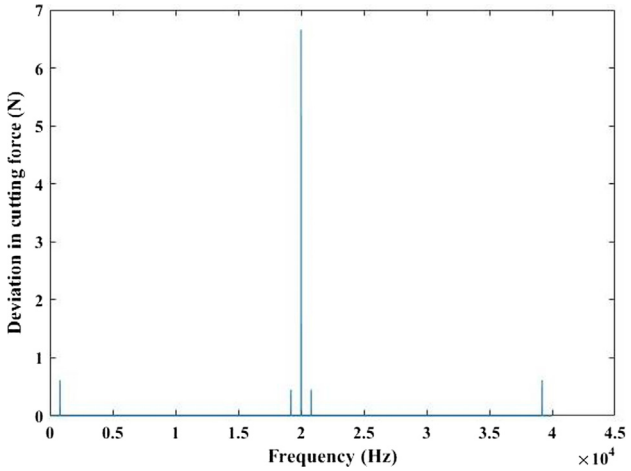

Fig. 4. FFT analysis of measured cutting force in Y direction (F_Y) at X_1 = 1500 RPM, X_2 = 100%, X_3 = 0.8 mm and X_4 = 70 mm/min.

Table 4
Experimental table with responses (cutting forces (F_X) and their standard deviation).

Exp. no.	X_1 (RPM)	X_2 (%)	X_3 (mm)	X_4 (mm/min)	F_X (N)	F_Y (N)	F_Z (N)	$\sigma(F_X)$	$\sigma(F_Y)$	$\sigma(F_Z)$
1	1875	100	0.6	50	6.69	3.54	2.02	1.33	0.708	0.438
2	2250	80	0.8	30	6.20	3.28	1.39	0.99	0.531	0.313
3	1500	80	0.8	70	8.82	4.68	2.49	1.43	0.774	0.457
4	1500	80	0.8	30	7.18	3.81	2.03	1.24	0.664	0.392
5	1875	60	0.6	50	8.26	4.38	2.02	1.10	0.591	0.349
6	1875	60	1.0	50	8.59	4.63	2.13	1.27	0.680	0.401
7	1500	80	0.4	70	8.23	4.36	2.42	1.34	0.715	0.422
8	2250	40	0.8	30	7.96	4.22	1.71	1.01	0.543	0.320
9	1875	60	0.6	50	7.59	4.02	1.82	1.15	0.615	0.363
10	1875	60	0.2	50	7.09	3.76	1.69	1.00	0.536	0.316
11	2250	80	0.8	70	7.54	3.99	1.74	1.11	0.593	0.350
12	2250	40	0.4	70	8.09	4.29	1.76	0.97	0.520	0.307
13	1500	40	0.4	70	8.56	4.54	2.19	1.16	0.621	0.366
14	1500	40	0.8	70	9.71	5.14	2.40	1.19	0.638	0.376
15	1125	60	0.6	50	8.22	4.41	2.29	1.28	0.607	0.358
16	1875	60	0.6	90	9.01	4.84	2.30	1.23	0.660	0.389
17	1875	20	0.6	50	8.46	4.49	1.79	0.97	0.519	0.306
18	1875	60	0.6	50	7.59	4.02	1.82	1.15	0.615	0.363
19	1875	60	0.6	50	8.07	4.27	2.04	1.11	0.596	0.352
20	1875	60	0.6	50	7.54	3.99	1.80	1.10	0.589	0.347
21	2625	60	0.6	50	5.95	3.21	1.08	0.82	0.436	0.257
22	2250	40	0.4	30	7.07	3.74	1.50	0.88	0.477	0.281
23	1875	60	0.6	10	6.58	3.55	1.37	0.97	0.522	0.308
24	1500	80	0.4	30	6.02	3.19	1.69	1.13	0.607	0.358
25	2250	40	0.8	70	8.43	4.47	1.85	0.99	0.532	0.314
26	1500	40	0.8	30	8.69	4.61	1.99	1.05	0.565	0.333
27	2250	80	0.4	30	5.29	2.80	1.09	0.99	0.533	0.314
28	1875	60	0.6	50	7.59	4.02	1.82	1.07	0.572	0.338
29	1500	40	0.4	30	6.99	3.70	1.62	1.04	0.555	0.327
30	1875	60	0.6	50	8.01	4.25	2.02	1.19	0.637	0.376
31	2250	80	0.4	70	6.42	3.40	1.39	1.08	0.578	0.341

comparing the obtained $F^{regression}$ (Fisher's value) value with the standard $F^{standard}$ value (for the model and lack of fit).

Regression models for all the responses were obtained, however, the developed model contained too many terms and some of these factors had insignificant effect on the responses. So, the developed model was further simplified by performing regression with all the significant (p values less than 0.05) factors. The ANOVA tables show that significant factors for all the responses are same, however their contributions are different. The regression equations with significant factors for all the responses were obtained, as given in Eqs. (1)–(6)

$$F_X = 0.33 + 0.00563X_1 + 0.01X_2 + 2.262X_3 + 0.0705X_4 - 0.0000012X_1^2 - 0.0000204X_1 \times X_2 - 0.0000214X_1 \times X_4 \quad (1)$$

$$F_Y = 0.32 + 0.00281X_1 + 0.0053X_2 + 1.232X_3 + 0.0374X_4 - 0.0000006X_1^2 - 0.000011 \times X_2 - 0.000011X_1 \times X_4 \quad (2)$$

$$F_Z = -0.73 + 0.00164X_1 + 0.02X_2 + 0.489X_3 + 0.0235X_4 - 0.0000003X_1^2 - 0.000011X_1 \times X_2 - 0.000008X_1 \times X_4 \quad (3)$$

$$\sigma(F_X) = -0.02 + 0.00062X_1 + 0.01X_2 + 0.202X_3 + 0.0090X_4 - 0.00000015X_1^2 - 0.000003X_1 \times X_2 - 0.000003X_1 \times X_4 \quad (4)$$

$$\sigma(F_Y) = -0.27 + 0.00059X_1 + 0.00535X_2 + 0.109X_3 + 0.005X_4 - 0.00000014X_1^2 - 0.0000018X_1 \times X_2 - 0.0000018X_1 \times X_4 \quad (5)$$

$$\sigma(F_Z) = -0.18 + 0.00036X_1 + 0.0033X_2 + 0.064X_3 + 0.0024X_4 - 0.000000084X_1^2 - 0.0000011X_1 \times X_2 - 0.0000011X_1 \times X_4 \quad (6)$$

where X_1 is the rotational speed of milling tool (RPM), X_2 is the ultrasonic power percentage (%), $X_3$is the axial depth of cut (mm), and $X_4$is the feed rate (mm/min). Tables 5 and 6 show that the F value of all regressions are greater than the standard F value and their 'lack of fit' are also insignificant (at 95% confidence level). Therefore, the regression equations can be considered as a predictive model for the cutting forces and their standard deviations in the considered range of factors.

The value of R^2 for all the responses (as it is less than 100%) shows the existence of error in the experimental data. This is due to the presence of noise in the data, which is mainly caused by machine vibrations. Due to this error, it is difficult to predict the responses accurately; however, a range can be predicted. Therefore, in order to estimate the range of responses, confidence interval can be calculated using$F_X \pm \delta(F_X)$, where $\delta(F_X)$ is given by [33].

$$\delta(F_X) = T_{(\alpha,DF)} \times \sqrt{V_e} \quad (7)$$

where V_e is the variance of error (mean of square (MS) of residual error in ANOVA table (Tables 5 and 6)) of the predictive model, T is the value from t distribution table for α (0.05 for 95% confidence level), and DF (degree of freedom = 30). The value of $\delta(F)$ for all the responses were calculated using Tables 5 and 6. In order to validate these statistical models, confirmation experiments (Table 7) were performed at three different set of process parameters and the responses were measured. The confirmation experiments (Table 7) show that the experimental findings lie within the predicted range. Thus, the developed model can be considered for the prediction of responses in the given range of process parameters.

5. Results and discussion

In order to understand the effect of process parameters on the mean cutting forces, main effect plots (Fig. 5) were obtained. Further, these plots were discussed to understand the effect of each parameter separately.

From Fig. 5 it can be seen that the main effect plots of F_X and F_Y are similar and slightly different fromF_Z. It is because both the cutting forces (F_X and F_Y) are the components of tangential (F_T) and radial (F_R) force acting on tooth during milling operation (at θ angular

Table 5
ANOVA table for mean cutting forces after removing insignificant terms.

Source	DF	Seq. SS			MS			F			P			R^2 (pred.) (%)		
		F_X	F_Y	F_Z	F_X	F_Y	F_Z	F_X	F_Y	F_Z	F_X	F_Y	F_Z	F_X	F_Y	F_Z
Regression	7	29.453	8.320	3.852	4.207	1.188	0.550	52.19	51.09	34.8	0.00	0.00	0.00	88.8	88.6	86.5
Linear	4	27.794	7.888	3.514												
Square	1	0.910	0.221	0.097												
Interaction	2	0.749	0.210	0.240												
Residual error	23	1.854	0.535	0.374	0.081	0.024	0.016									
Lack of fit	17	1.324	0.386	0.190				0.88	0.91	0.39	0.62	0.59	0.91			
Pure error	6	0.530	0.149	0.174												
Total	30	31.307	8.855	4.216												

$F^{standard}_{0.05,7,23} = 2.488$, $F^{standard}_{0.05,17,23} = 2.139$ for all three forces (F_X, F_Y and F_Z) the $F^{regression} > F^{standard}_{0.05,7,23}$ and $F^{lackoffit} < F^{standard}_{0.05,7,23}$ this shows that model for these forces are adequate and lack of fit are insignificant

position of tooth) (Eq. (7) [35]. Therefore, as the tangential and radial forces vary with process parameters, both these forces follow the same trend. However, the effect of process parameters on F_Z is slightly different as can be seen from Fig. 5j.

$$\left.\begin{aligned} F_X &= F_T\cos(\theta) + F_R\sin(\theta) \\ F_y &= F_R\cos(\theta) - F_T\sin(\theta) \end{aligned}\right\} \quad (8)$$

From the main effect plots (Fig. 5a and e) it can be seen that cutting forces decrease with increase in tool rotational speed. It happens due to reduction in uncut chip thickness (given as feed rate per tooth), which is directly proportional to the cutting forces [36]. Furthermore, with the increase in rotational speed the cutting velocity increases which causes higher shear rate. This generates heat in the shear zone and causes reduction in shear strength of the material due to thermal softening [37]. Thus, an increase in the rotational speed results in the reduction of cutting force.

The main effect plot (Fig. 5b and f) shows that as the ultrasonic power percentage (UP) increases the cutting force decreases. To evaluate the intermittent cutting effect, in the present case harmonic analysis was performed (Fig. 6a) and deformation vector at the tool tip was evaluated.

The result of harmonic analysis (Fig. 6b and c) shows that the direction of deformation vector at the cutting tip follows the helix profile. Furthermore, V_{ul} and their respective contact ratio (Eq. (10) was evaluated by using simulation results and Eq. (9). The calculation results show that, as the UP increases the cutting ratio decreases (from 0.75 at 20% to 0.59 at 100%) which further results in decrease in the cutting forces [18]. In addition to that, during UAM, ultrasonic energy gets transmitted to the workpiece, which causes acoustic softening of the workpiece and results in lowering of shear strength (occurs in Al and Al alloys) [38,39].

$$V_{ul} = 2\pi af \times cos(2\pi ft) \quad (9)$$

$$r_c = 1 - \frac{1}{\pi}\left(\cos^{-1}\left(\frac{V_n}{max\ \ of\ \ V_{ul\_t}}\right)\right) \quad (10)$$

where f, a, t, V_{ul}, r_c *and* V_n are frequency of vibration, amplitude of vibration (deformation of the cutting tip), time, velocity due to ultrasonic vibration, contact ratio and velocity due to tool rotation respectively. Additionally Fig. 5(j) shows that F_Z initially increases and then decreases which is mainly due to due to the axial vibration which applies additional discontinuous force in axial direction. However, with further increase in UP, the intermittent cutting effect starts dominating and results in drop in F_Z. Due to the presence of this additional axial force the drop in the F_Z is not as significant as in F_X and F_Y.

It can also be seen from the main effect plots (Fig. 5c and g) that, with the increase in axial depth of cut (DOC) cutting force increases. It is because with the increase in DOC, the width of uncut chip increases, which causes increase in cutting force. From Fig. 5d and h it is clear that cutting forces increase with increase in the feed rate. It is due to the increased uncut chip thickness (feed rate per tooth), that causes increase in cutting force [36].

The main effect plots of F_Z (Fig. 5i–l) show that, except UP all the parameters have similar trends as followed by F_X and F_Y. This variation can be because of the impact that occurs between the tool tip and workpiece surface which diminishes the effect of intermittent cutting.

The ANOVA results showed that, apart from the individual effect of the process parameters, interactions ((a) UP & RPM and (b) RPM &feed rate) also have a significant effect on the responses. Therefore, to understand the simultaneous effect of two parameters, 3D surface plots and their 2D graphs were obtained using the regression Eq. (1).

Fig. 7a and b show the interaction plot of rotational speed and ultrasonic power on cutting force (F_X). It can be seen from the graph (Fig. 7b) that at higher UP (100%) with an increase in the rotation speed the cutting forces decrease rapidly, however at lower UP the drop is not that sharp. In order to investigate this result, cutting ratio was evaluated for all the cutting conditions. From the result it was found that at higher UP (due to high V_{ul}) (~1.2 m/s), the contact ratio increases very slightly (from 0.56 at 1125 RPM (~0.19 m/s) to 0.62 at 2625 RPM (~0.43 m/s),). Therefore, at 100% UP the effect of intermittent cutting does not diminish with increase in rotational speed. However, at lower UP (20%), the contact ratio increases rapidly (from 0.63 at 1125 RPM (~0.19 m/s), to 0.87 at 2625 RPM (~0.43 m/s)) and causes reduction in the intermittent cutting effect. Due to the reduction in the intermittent cutting effect the cutting force first increases slightly. However, further rise in rotational speed increases the chip thinning and thermal softening effect starts dominating which further results in reduction in cutting forces. Therefore, at higher UP (100%) the effects associated to UP and rotational speed act simultaneously and causes rapid drop in the cutting force. However, at lower UP, due to the decrease in intermittent cutting effect only effects associated rotational speed occurs and results in a small drop in the cutting force.

Fig. 8a shows the interaction plot of feed rate and rotational speed for F_X. It can be seen from the graph (Fig. 8b) that at lower rotational speed (1125 RPM) with an increase in feed rate the cutting force increases rapidly. It may be due to the increase in chip thickness [36] with feed rate that causes higher shear force during milling. However, at higher rotational speed (2625 RPM) the rate of increase in cutting force is not that sharp. The reason may be attributed to the fact that, at higher rotational speed the generation of heat in the shear zone is higher [37] which causes thermal softening and reduces the material shear strength and cutting force.

As explained F_X and F_Y are dependent on F_T and F_R (Eq. (7), due to which the interaction effects for F_Y are similar to F_X. So, in order to avoid redundancy, only interactions for F_X are discussed in this paper. Apart from F_X and F_Y the parameters also have simultaneous effect on F_Z as seen in Eq. (3). These interaction effects were explained by plotting 3D surfaces and their 2D plots (Figs. 9 and 10).

Table 6
ANOVA table for standard deviation in the cutting forces after removing insignificant terms.

Source	DF	Seq. SS			MS			F			P			R^2 (pred.) (%)		
		$\sigma(F_X)$	$\sigma(F_Y)$	$\sigma(F_Z)$	$\sigma(F_X)$	$\sigma(F_Y)$	$\sigma(F_Z)$	$\sigma(F_X)$	$\sigma(F_Y)$	$\sigma(F_Z)$	$\sigma(F_X)$	$\sigma(F_Y)$	$\sigma(F_Z)$	$\sigma(F_X)$	$\sigma(F_Y)$	$\sigma(F_Z)$
Regression	7	0.730	0.203	0.074	0.077	0.029	0.428	49.43	48.08	49.85	0.00	0.00	0.00	83.2	82.9	82.7
Linear	4	0.671	0.187	0.067												
Square	1	0.035	0.010	0.004												
Interaction	2	0.023	0.006	0.003												
Residual error	23	0.048	0.014	0.007	0.0021	0.0006	0.0003									
Lack of fit	17	0.041	0.011	0.005				1.87	1.86	0.66	0.22	0.23	0.77			
Pure error	6	0.008	0.002	0.002												
Total	30	0.778	0.221	0.081												

$F^{standard}_{0.05,7,23}$ = 2.488, $F^{standard}_{0.05,17,23}$ = 2.139 for standard deviation of forces ($\sigma(F_X)$, $\sigma(F_Y)$ and$\sigma(F_Z)$) the $F^{regression} > F^{standard}_{0.05,7,23}$ and $F^{lackoffit} < F^{standard}_{0.05,7,23}$ this shows that model for standard deviation of forces are adequate and lack of fit are insignificant

where MS: mean of square; Seq. SS: sequential sum of squares; DF: degree of freedom; F: Fisher's value.

Table 7
Confirmation experiments for the developed model.

	Experiment 1		Experiment 2		Experiment 3	
Cutting forces	RPM-1500 UP-100 DOC-1 Feed rate-30		RPM-2200 UP-90 DOC-0.3 Feed rate-20		RPM-1875 UP-40 DOC-0.8 Feed rate-80	
	F(N)	$\sigma(F)$	F(N)	$\sigma(F)$	F(N)	$\sigma(F)$
Predicted F_X	7.35 ± 0.58	1.42 ± 0.10	4.73 ± 0.58	1.01 ± 0.10	9.66 ± 0.58	1.20 ± 0.10
Experiment F_X	7.92	1.49	5.27	0.91	10.04	1.12
Predicted F_Y	3.91 ± 0.32	0.76 ± 0.07	2.50 ± 0.32	0.53 ± 0.07	5.17 ± 0.32	0.64 ± 0.07
Experiment F_Y	4.22	0.83	2.79	0.47	5.44	0.59
Predicted F_Z	2.33 ± 0.26	0.44 ± 0.05	1.28 ± 0.26	0.31 ± 0.05	2.85 ± 0.26	0.38 ± 0.05
Experiment F_Z	2.53	0.49	1.49	0.26	3.07	0.34

As seen from the 2D plot, at higher UP (100%), cutting force (F_Z) decreases rapidly with increase in RPM, however, at lower UP (20%) the drop is not that sharp. It may be because at higher UP, the intermittent cutting and acoustic softening effect occur simultaneously causing rapid decrease in average cutting force. However, at lower UP, intermittent cutting effect diminishes and only the effect of RPM occurs and causes a steady drop in cutting force.

It can be seen from Fig. 10b that at higher RPM the cutting force increases gradually with increase in feed rate. This is due to the thermal softening occurring at the shear zone due to higher shear rate. Apart from the cutting forces, the parameters also affect the standard deviation in the cutting force. So, in order to evaluate the effect of cutting parameters the main effect plots were obtained.

As the standard deviation in the cutting force depends on the width and uncut chip thickness [40], the trends in the main effect plot (Fig. 10) of most of the parameters are slightly similar to the cutting forces. The main effect plots (Fig. 11a, e and i) show that standard deviation in cutting force decreases with increase in rotational speed. It is because the standard deviation in cutting force is proportional to the uncut chip thickness [40]. In addition, cutting velocity causes heat generation in the shear zone [37] which reduces the shear strength. So, as the rotational speed increases the simultaneous effect reduces the standard deviation in cutting force. From the main effect plots (Fig. 11b, f and j) it can be seen that the standard deviation of cutting forces increases with increase in UP. This is due to the intermittent cutting effect occurring at the cutting zone. During engagement between tool and workpiece impact occurs, which causes sudden rise in cutting forces. As UP increases the intensity of this impact increases which further results in higher impulsive forces. This impulsive force keeps increasing with amplitude due to increase in$\frac{dV}{dt}$ (Eq. (11) which causes rise in maximum value of cutting forces. This results in higher variation in the cutting forces which further causes increase in the standard deviation.

$$\left(\frac{dV}{dt} = 4a(\pi f)^2 \times cos(2\pi ft)\right) \tag{11}$$

From Fig. 11c, g and k it can be seen that the standard deviation also increases with increase in DOC. This is because the cutting force and its standard deviation are directly proportional to the width of uncut chip [37]. From the main effect plot (Fig. 11d, h and l) it can also be seen that standard deviation increases with increase in feed rate. Due to this, the uncut chip thickness and standard deviation in the cutting force increases. It is because the standard deviation in cutting force is proportional to the uncut chip thickness (feed rate per tooth) [40]. As already explained that both $F_X$andF_Y forces are the components of $F_T$andF_R, so the main effect plot and the interactions of both $\sigma(F_X)$ and$\sigma(F_Y)$ are also similar. Therefore in order to avoid redundancy,

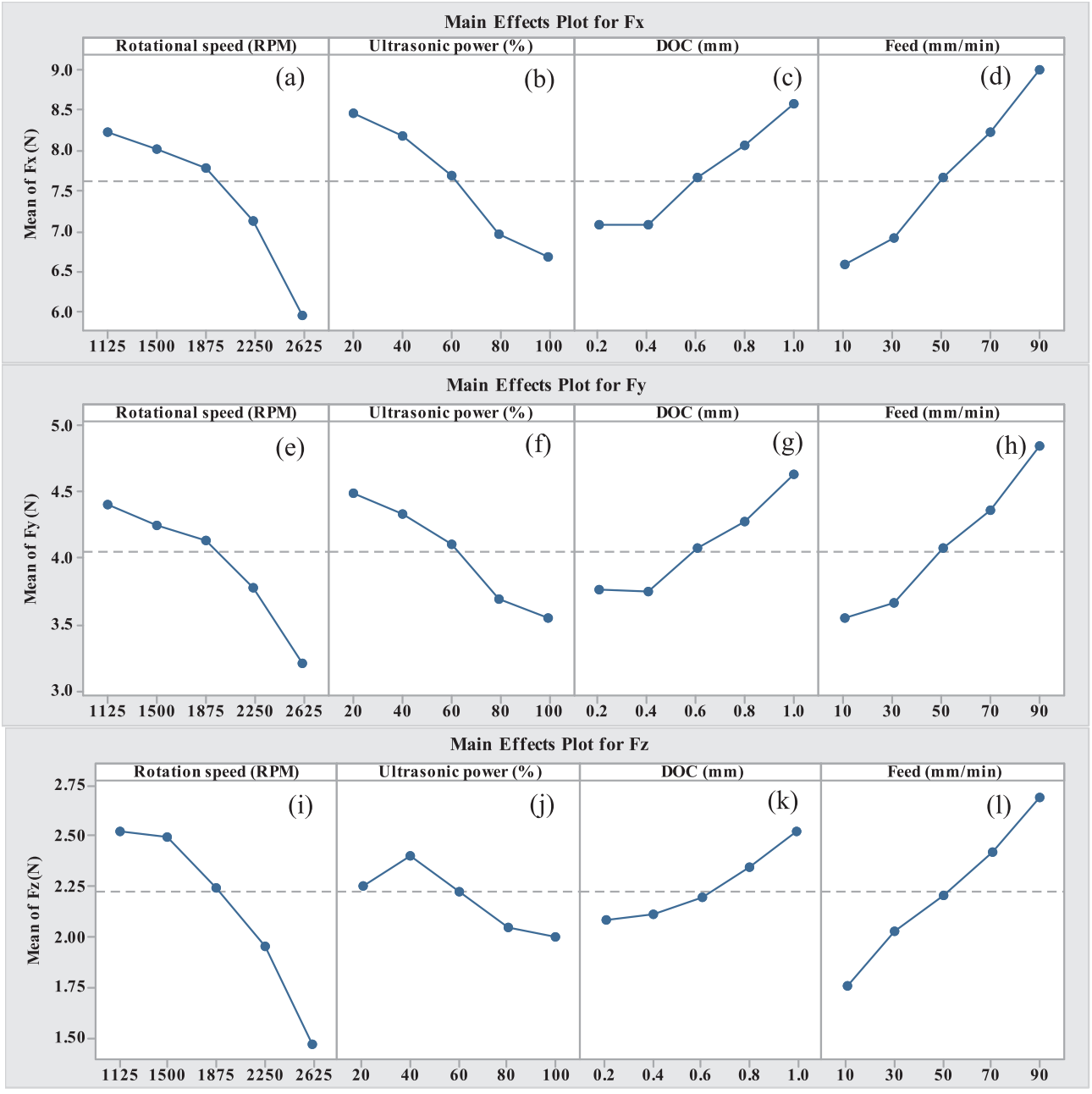

Fig. 5. Main effect plots for cutting forces (F_X, F_Y andF_Z) with respect to the process parameters.

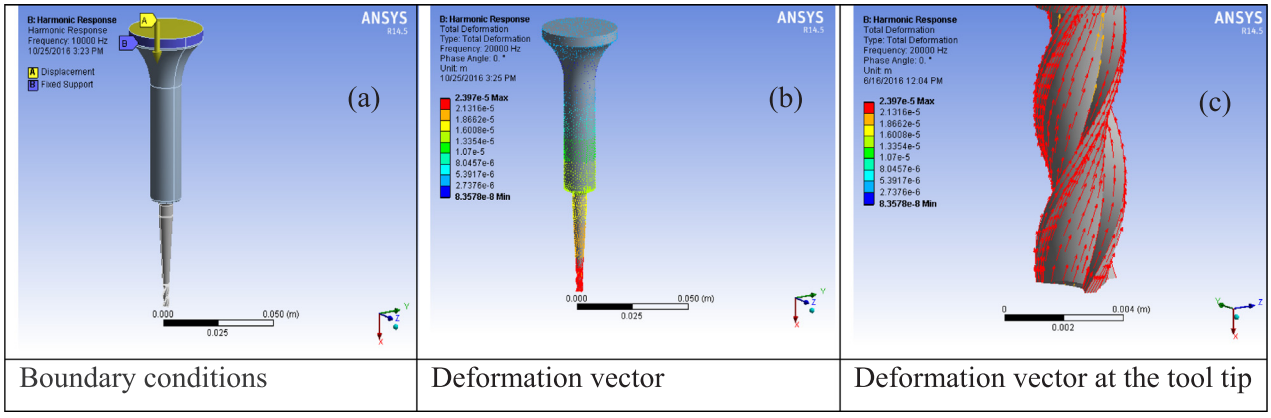

Fig. 6. Harmonic analysis for the evaluation of deformation vector at the tool tip.

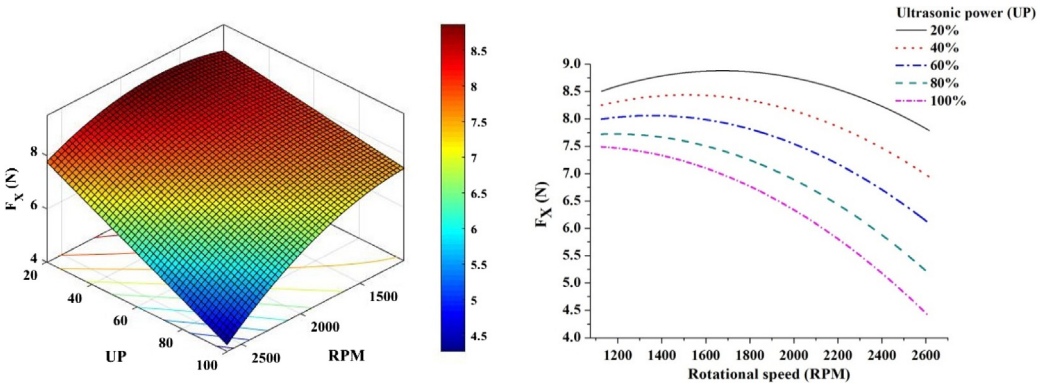

(a) Surface plot of F_X with respect to ultrasonic power and rotational speed

(b) 2D illustration of surface plot at five different intervals

Fig. 7. Simultaneous effect of ultrasonic power and rotational speed on F_X (at DOC = 0.6 mm & feed rate = 50 mm/min).

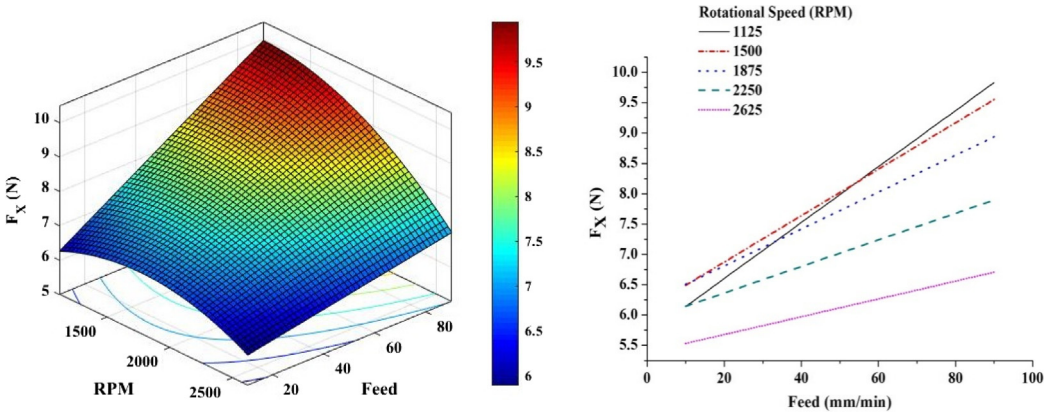

(a) Surface plot of F_X with respect to feed rate and rotational speed

(b) 2D illustration of surface plot at five different intervals

Fig. 8. Simultaneous effect of feed rate and rotational speed on F_X (at DOC = 0.6 mm & UP = 60%).

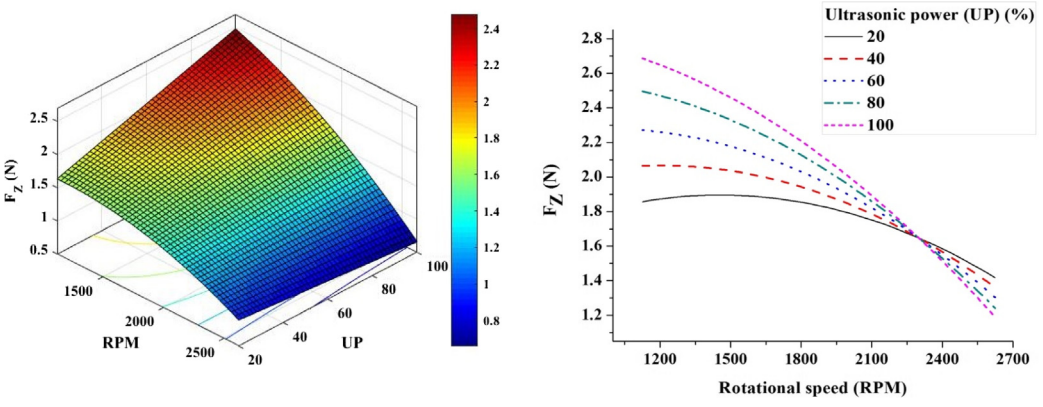

(a) Surface plot of F_Z with respect to ultrasonic power and rotational speed

(b) 2D illustration of surface plot at five different intervals

Fig. 9. Simultaneous effect of ultrasonic power and rotational speed on F_Z (at DOC = 0.6 mm & feed rate = 50 mm/min).

effect of factors on $\sigma(F_X)$ has been discussed. Furthermore, to evaluate the simultaneous effect of process parameters, 3D surface and their 2D plots were obtained using Eq. (4).

Fig. 12a shows the simultaneous effect of UP and RPM on$\sigma(F_X)$. It can be seen from the 2D plot (Fig. 12b) that at lower rotational speed (1125 RPM) $\sigma(F_X)$ increases rapidly with increase in UP. It may be due to the occurrence of intermittent cutting that causes variation in cutting force from 0 to the maximum value. However, at higher rotation speed the $\sigma(F_X)$ increases steadily with increase in feed rate. This is because at higher rotational speed the heat generation at the shear zone is high (due to higher shear rate) which causes lowering of shear strength of material [37] and results in steady rise in $\sigma(F_X)$ with UP.

From Fig. 13a and b, it is clear that at lower rotational speed (1125 RPM) with an increase in feed rate $\sigma(F_X)$ increases rapidly. However, at

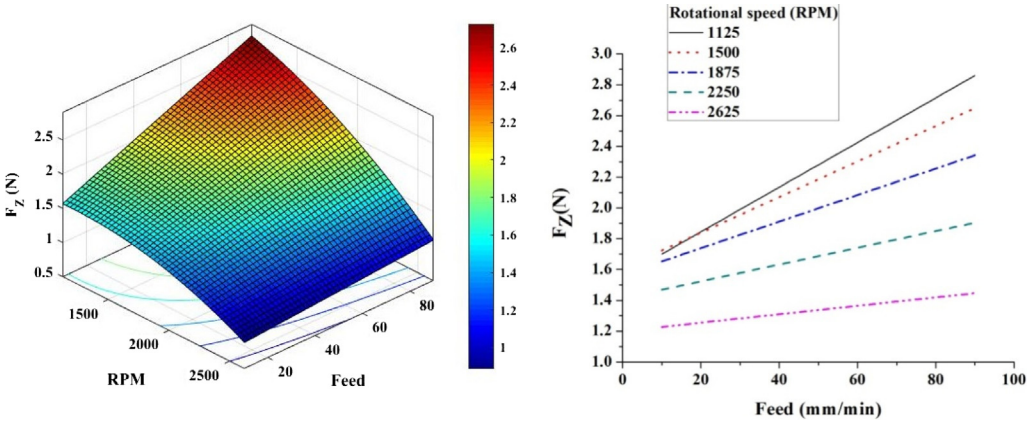

(a) Surface plot of F_Z with respect to feed rate and rotational speed

(b) 2D illustration of surface plot at five different intervals

Fig. 10. Simultaneous effect of feed rate and rotational speed on F_Z (at DOC = 0.6 mm & UP = 60%).

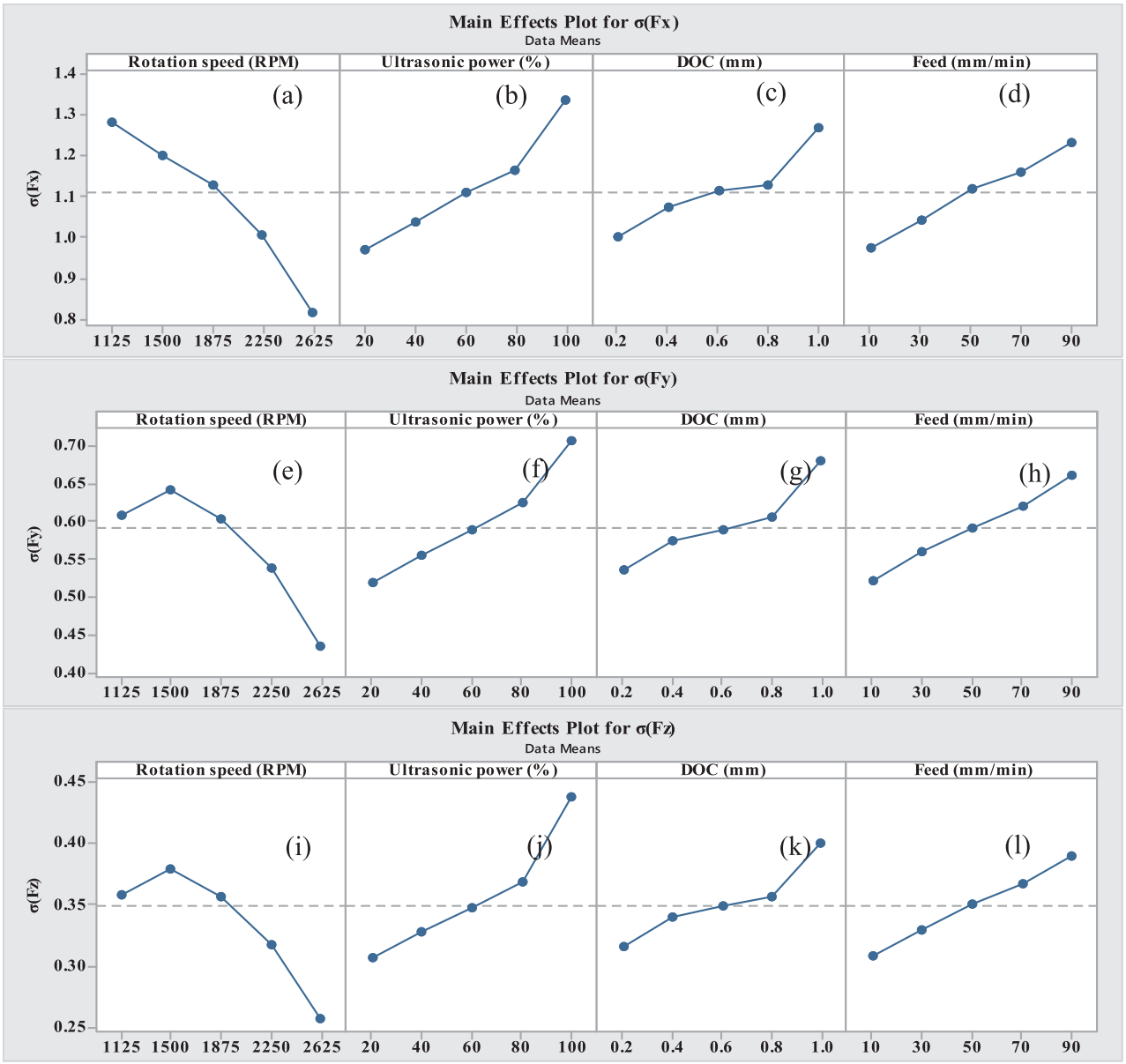

Fig. 11. Main effect plots for standard deviation in cutting forces ($\sigma(F_X)$, $\sigma(F_Y)$and$\sigma(F_Z)$) with respect to the machining parameters.

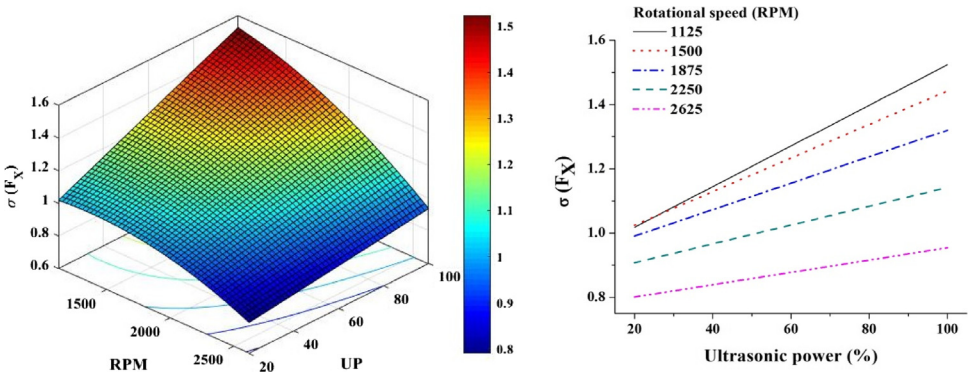

(a) Surface plot of $\sigma(F_X)$ with respect to ultrasonic power and rotational speed

(b) 2D illustration of surface plot at five different intervals

Fig. 12. Simultaneous effect of ultrasonic power and rotational speed on $\sigma(F_X)$ (at DOC = 0.6 mm & feed rate = 50 mm/min).

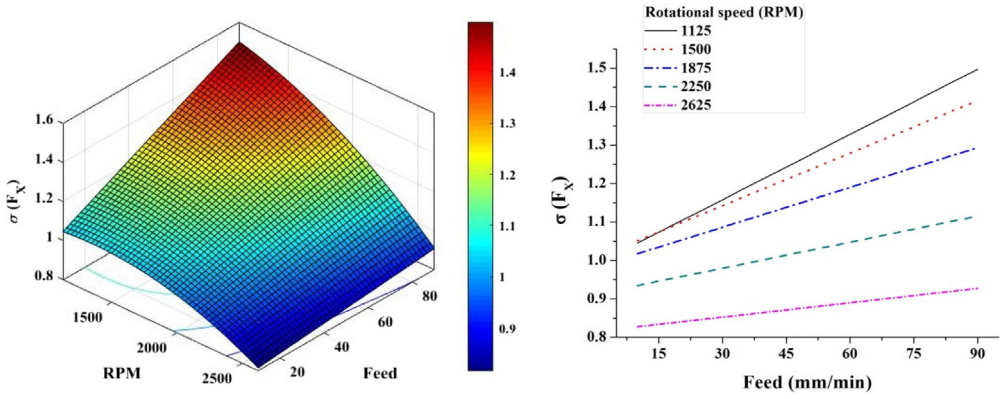

(a) Surface plot of $\sigma(F_X)$ with respect to feed rate and rotational speed

(b) 2D illustration of surface plot at five different intervals

Fig. 13. Simultaneous effect of feed rate and rotational speed on $\sigma(F_X)$ (at DOC = 0.6 mm & UP = 60%).

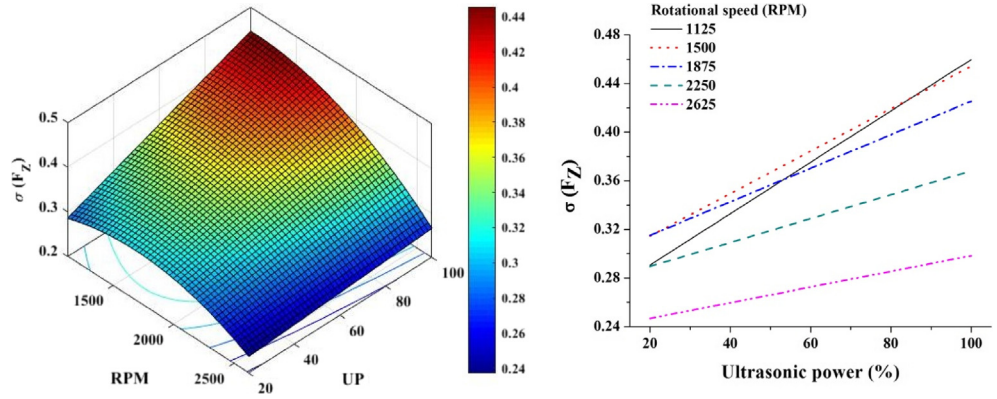

(a) Surface plot of $\sigma(F_Z)$ with respect to ultrasonic power and rotational speed

(b) 2D illustration of 2D illustration of surface plot at five different intervals

Fig. 14. Simultaneous effect of ultrasonic power and rotational speed on $\sigma(F_Z)$ (at DOC = 0.6 mm & feed rate = 50 mm/min).

higher rotational speed (2625 RPM) the increase is not that steep. It may be because of thermal softening occurring at the shear zone due to higher shear rate [37].

It can be seen from Fig. 14a and b that at lower rotational speed (1125 RPM) $\sigma(F_Z)$ increases with increase in UP. It may be due to impulsive force generated by the impact occurring between the tool tip and workpiece. Furthermore, with the increase in UP the impulsive force increases which causes rise in$\sigma(F_Z)$. However, at higher RPM the thermal softening occurs [37], which causes lower $\sigma(F_Z)$ with increase in UP.

From Fig. 15b it can be seen that the trend of the interaction for $\sigma(F_Z)$ is similar to$\sigma(F_X)$. This may be because of thermal softening that occurs at higher cutting speed [37]. The above results show that trends for all the parameters and their interactions are almost the same for all

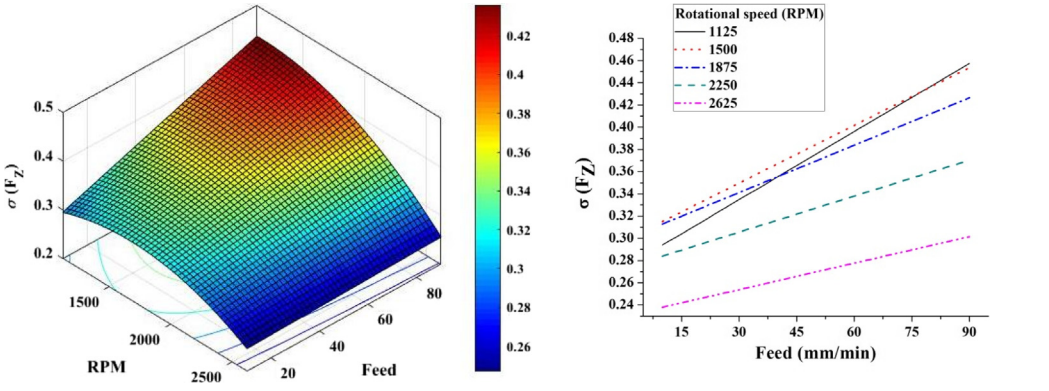

(a) Surface plot of $\sigma(F_Z)$ with respect to feed rate and rotational speed

(b) 2D illustration of surface plot at five different intervals

Fig. 15. Simultaneous effect of feed rate and rotational speed on $\sigma(F_Z)$ (at DOC = 0.6 mm & UP = 60%).

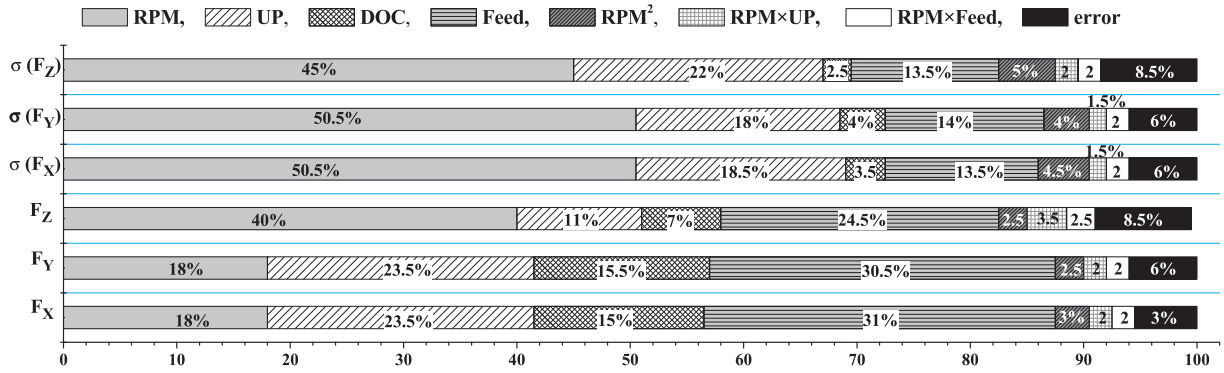

Fig. 16. Bar chart for the percentage contribution of all effective parameters on the responses.

Table 8
Constants for mean cutting forces (F) and their standard deviations $\sigma(F)$ for the developed semi-empirical model.

UP %	Constants	F_X	F_Y	F_Z	$\sigma(F_X)$	$\sigma(F_Y)$	$\sigma(F_Z)$
20%	C	10.4	8.28	2.62	8.37	2.29	2.61
	a	0.12	0.15	0.15	0.8	0.8	0.8
	b	0.08	0.11	0.133	0.117	0.117	0.129
	c	0.08	0.13	0.1	0.33	0.25	0.24
40%	C	10.9	9.84	2.05	8.97	2.95	2.36
	a	0.12	0.15	0.15	0.8	0.8	0.8
	b	0.08	0.096	0.192	0.0876	0.129	1.223
	c	0.1	0.15	0.11	0.32	0.28	0.22
60%	C	10.2	7.50	1.93	8.13	2.76	2.1
	a	0.14	0.2	0.15	0.8	0.8	0.8
	b	0.08	0.0986	0.218	0.082	0.143	0.117
	c	0.11	0.12	0.11	0.3	0.28	0.3
80%	C	38	8.77	55.02	8.93	4.46	1.1
	a	0.22	0.2	0.11	0.8	0.8	0.8
	b	0.15	0.048	0.25	0.074	0.0657	0.085
	c	0.25	0.12	0.5	0.3	0.3	0.32
100%	C	18	8.28	41.39	65.38	3.72	0.14
	a	0.3	0.2	0.14	0.8	0.8	0.8
	b	0.15	0.039	0.344	0.09	0.967	0.069
	c	0.25	0.12	0.57	0.57	0.28	0.32

the responses. However, the percentage contribution of all the parameters for each response is different. Fig. 16 shows the percentage contribution of each parameter for all output responses. It can also be seen that percentage contribution of all the parameters are the same for F_X and F_Y and is mostly affected by feed rate followed by UP. However, the percentage contribution for all the SD in cutting forces is the same and is mainly affected by rotational speed followed by UP. Furthermore, the percentage contribution chart (Fig. 16) was plotted for all the responses (using ANOVA result).

As the developed regression model has high goodness of fit the same can be used to generate an semi-empirical model giving more physical feel. However, it was not possible to obtain a general model. Hence, three different models of the following form were fitted at five different ultrasonic power percentage (UP) (%):

$$F = C\frac{(\text{Axial depth of cut},\ X_3)^a \times (\text{Feed rate},\ X_4)^b}{(\text{Rotational speed},\ X_1)^c} \tag{12}$$

where F is the response (mean and standard deviation in the cutting forces) and C, a, b, c are the constants (given in Table 8)

From these equations, it is clear that the cutting forces and their standard deviations always increases with increasing feed rate and axial depth of cut. However, the increase in rotational speed causes decrease in the UAM forces.

In order to find the set of process parameters which result in minimum forces with minimum deviation, the generated models were optimized using “multi-objective genetic algorithm tool box” in MatLab15b. The set of process parameters at which the models were optimized are shown in Table 8. Due to the opposite effect of ultrasonic power on mean and standard deviation of cutting force, the optimum parameters have been found to be different. Therefore, in order to achieve an ideal value of both mean and standard deviation, multi-objective optimization using genetic algorithm has been performed. Mean cutting force (of X direction) (F_X) and its standard deviations (of X direction)($\sigma(F_X)$) have been considered as objective 1 and 2 for the multi-objective optimization. Optimized parameters were obtained

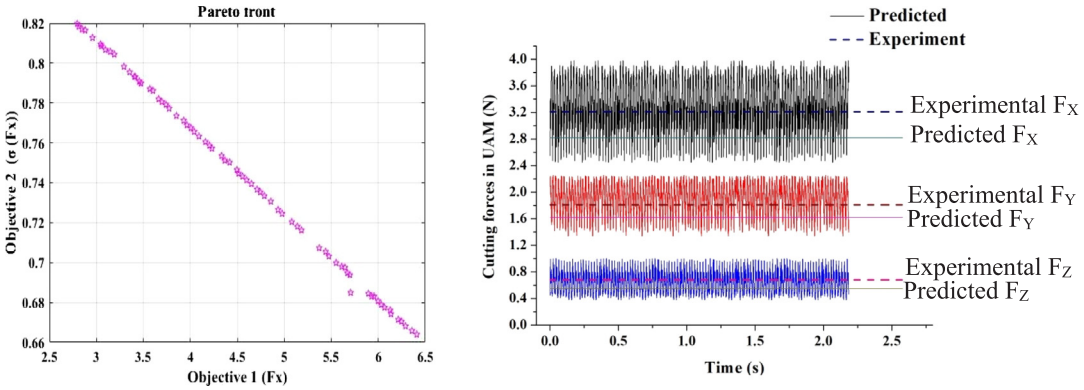

Fig. 17. a. Pareto front for cutting force F_X (objective 1) and its standard deviation$\sigma(F_X)$ (objective 2), b. Cutting forces (predicted and experimental) for UAM process at optimized parameters (experiment 1 in Table 7).

Table 9
Experiments at optimized parameters.

Optimized value of parameters from Pareto front data	Experiment 1		Experiment 2		Experiment 3	
	Optimum parameters for minimum cutting forces		Optimum parameters for minimum standard deviation in cutting forces			
Parameters for UAM experiments	RPM-2625 UP-100 DOC-0.2 Feed rate-10		RPM-2625 UP-20 DOC-0.2 Feed rate-10		RPM-2625 UP-60 DOC-0.2 Feed rate-10	
Cutting forces	F(N)	$\sigma(F)$	F(N)	$\sigma(F)$	F(N)	$\sigma(F)$
Predicted F_X	2.81 ± 0.58	0.81 ± 0.10	6.28 ± 0.58	0.66 ± 0.10	4.52 ± 0.58	0.73 ± 0.10
Experiment F_X	3.29	0.89	5.73	0.58	4.83	0.81
Predicted F_Y	1.50 ± 0.32	0.64 ± 0.07	3.35 ± 0.32	0.35 ± 0.07	2.43 ± 0.32	0.38 ± 0.07
Experiment F_Y	1.81	0.71	3.09	0.29	2.68	0.43
Predicted F_Z	0.51 ± 0.26	0.34 ± 0.05	1.85 ± 0.26	0.21 ± 0.05	1.18 ± 0.26	0.22 ± 0.05
Experiment F_Z	0.78	0.40	1.61	0.17	1.38	0.26

from the Pareto front [41] generated (Fig. 17a) after multi-objective optimization of regression equations for F_X(objective 1) and$\sigma(F_X)$ (objective 2) (Fig. 17a). Further the experiments were performed at optimized parameters (selected from the pareto front data) to ensure the accuracy of the developed model in optimum conditions.

The experimental results (Table 8) show that the precision of the developed regression model for mean of cutting forces and standard deviation have good precision and accuracy. Fig. 17a shows the cutting forces and the comparison of the mean cutting forces (predicted and experimental) for experiment 1 (Table 9). It may be due to the presence of noise in the data caused by machine vibration, noise in the dynamometer response, etc.

6. Conclusions

In the present study, a statistical model has been developed for ultrasonic assisted milling process. The developed model evaluates the effect of process parameters on cutting forces and deviation in the cutting forces. The model has been verified by performing confirmation experiments on intermediate and optimized parameters. The cutting kinematics has also been studied by simulating the milling tool with axial ultrasonic vibrations. The following conclusions can be made from the present work:

1. The simulation results confirmed the existence of torsional vibration (in milling tool with helix angle) which results in intermittent cutting and thus helps lower the average cutting force.
2. The axial ultrasonic vibration reduces the average cutting force and increases its standard deviation.
3. The behavior of all the parameters except ultrasonic power is almost the same for all the responses.
4. The effect of all the parameters on F_X and F_Y are similar and different forF_Z; however the behavior of parameters on the standard deviation ofF_X, F_Y and $F_Z$are similar.
5. The most effective parameter for main cutting forces (F_X and F_Y) is feed rate (~31%) followed by ultrasonic power; however, their standard deviation is affected by rotational speed (~50%).
6. Working at "RPM = 2625, UP = 100%, DOC = 0.2 mm, and feed rate = 10 mm/min" resulted in minimum UAM force. However working at "RPM = 2625, UP = 20%, DOC = 0.2 mm, and feed rate = 10 mm/min" results in minimum standard deviation.

Acknowledgement

The financial support offered by the DST (India)-EPSRC (UK) sponsored project entitled 'MAST: Modeling of Advanced Materials for Simulation of Transformative Manufacturing Processes' (Grant identification: DST/RC-UK/14-AM/2012) is gratefully acknowledged.

References

[1] A. Ginting, M. Nouari, Experimental and numerical studies on the performance of alloyed carbide tool in dry milling of aerospace material, Int. J. Mach. Tools Manuf. 46 (2006) 758–768, https://doi.org/10.1016/j.ijmachtools.2005.07.035.
[2] M. Soković, K. Mijanović, Ecological aspects of the cutting fluids and its influence on quantifiable parameters of the cutting processes, J. Mater. Process. Technol. 109 (2001) 181–189, https://doi.org/10.1016/S0924-0136(00)00794-9.
[3] B. Wang, Z. Liu, G. Su, Q. Song, X. Ai, Investigations of critical cutting speed and ductile-to-brittle transition mechanism for workpiece material in ultra-high speed machining, Int. J. Mech. Sci. 104 (2015) 44–59, https://doi.org/10.1016/j.ijmecsci.2015.10.004.
[4] J. Tlusty, Dynamics of high-speed milling, J. Eng. Ind. 108 (1986) 59–67.
[5] Y. Liu, Z. Liu, Q. Song, B. Wang, Development of constrained layer damping tool-holder to improve chatter stability in end milling, Int. J. Mech. Sci. 117 (2016) 299–308, https://doi.org/10.1016/j.ijmecsci.2016.09.003.
[6] P.H. Lee, J.S. Nam, C. Li, S.W. Lee, An experimental study on micro-grinding process with nanofluid minimum quantity lubrication (MQL), Int. J. Precis. Eng. Manuf. 13 (2012) 331–338, https://doi.org/10.1007/s12541-012-0042-2.
[7] Y. Zhang, C. Li, D. Jia, D. Zhang, X. Zhang, Experimental evaluation of MoS2 nanoparticles in jet MQL grinding with different types of vegetable oil as base oil, J. Clean. Prod. 87 (2015) 930–940, https://doi.org/10.1016/j.jclepro.2014.10.027.
[8] N.R. Dhar, M.T. Ahmed, S. Islam, An experimental investigation on effect of minimum quantity lubrication in machining AISI 1040 steel, Int. J. Mach. Tools Manuf. 47 (2007) 748–753, https://doi.org/10.1016/j.ijmachtools.2006.09.017.
[9] M. Rahman, A. Senthil Kumar, M.U. Salam, Experimental evaluation on the effect of minimal quantities of lubricant in milling, Int. J. Mach. Tools Manuf. 42 (2002) 539–547, https://doi.org/10.1016/S0890-6955(01)00160-2.
[10] M.M. Abootorabi Zarchi, M.R. Razfar, A. Abdullah, Influence of ultrasonic vibrations on side milling of AISI 420 stainless steel, Int. J. Adv. Manuf. Technol. 66 (2013) 83–89, https://doi.org/10.1007/s00170-012-4307-9.

[11] M.M. Abootorabi Zarchi, M.R. Razfar, A. Abdullah, Investigation of the effect of cutting speed and vibration amplitude on cutting forces in ultrasonic-assisted milling, Proc. Inst. Mech. Eng. Part B J. Eng. Manuf. 226 (2012) 1185–1191, https://doi.org/10.1177/0954405412439666.
[12] J.H. Ko, S.W. Tan, Chatter marks reduction in meso-scale milling through ultrasonic vibration assistance parallel to tooling's axis, Int. J. Precis. Eng. Manuf. 14 (2013) 17–22, https://doi.org/10.1007/s12541-013-0003-4.
[13] H. Ding, S.J. Chen, K. Cheng, Two-dimensional vibration-assisted micro end milling: cutting force modelling and machining process dynamics, Proc. Inst. Mech. Eng. Part B – J. Eng. Manuf. 224 (2010) 1775–1783, https://doi.org/10.1243/09544054jem1984.
[14] R.C. Skelton, Turning with an oscillating tool, Int. J. Mach. Tool Des. Res. 8 (1968) 239–259, https://doi.org/10.1016/0020-7357(68)90014-0.
[15] D.E. Brehl, T.A. Dow, Review of vibration-assisted machining, Precis. Eng. 32 (2008) 153–172, https://doi.org/10.1016/j.precisioneng.2007.08.003.
[16] X.H. Shen, J.H. Zhang, H. Li, J.J. Wang, X.C. Wang, Ultrasonic vibration-assisted milling of aluminum alloy, Int. J. Adv. Manuf. Technol. 63 (2012) 41–49, https://doi.org/10.1007/s00170-011-3882-5.
[17] X. Shen, J. Zhang, T. Yin, C. Dong, A Study on cutting force in micro end milling with ultrasonic vibration, Adv. Mater. Res. 101 (2010) 1910–1914, https://doi.org/10.4028/www.scientific.net/AMR.97-101.1910.
[18] C. Nath, M. Rahman, Effect of machining parameters in ultrasonic vibration cutting, Int. J. Mach. Tools Manuf. 48 (2008) 965–974, https://doi.org/10.1016/j.ijmachtools.2008.01.013.
[19] A. Suárez, F. Veiga, L.N.L. de Lacalle, R. Polvorosa, S. Lutze, A. Wretland, Effects of ultrasonics-assisted face milling on surface integrity and fatigue life of Ni-Alloy 718, J. Mater. Eng. Perform. 25 (2016) 5076–5086, https://doi.org/10.1007/s11665-016-2343-6.
[20] K.-M. Li, S.-L. Wang, Effect of tool wear in ultrasonic vibration-assisted micro-milling, Proc. Inst. Mech. Eng. Part B J. Eng. Manuf. 228 (2013) 847–855, https://doi.org/10.1177/0954405413510514.
[21] E. Uhlmann, F. Protz, B. Stawiszynski, S. Heidler, Ultrasonic assisted milling of reinforced plastics, Proc. CIRP 66 (2017) 164–168, https://doi.org/10.1016/j.procir.2017.03.278.
[22] J.H. Ko, K.C. Shaw, H.K. Chua, R.M. Lin, Cusp error reduction under high speed micro/meso-scale milling with ultrasonic vibration assistance 12 (2011) 15–20. 10.1007/s12541-011-0002-2.
[23] P. Sarvi Hampa, M.R. Razfar, M. Malaki, A. Maleki, The role of dry aero-acoustical lubrication and material softening in ultrasonically assisted milling of difficult-to-cut AISI 304 Steels, Trans. Indian Inst. Met. 68 (2014) 43–49, https://doi.org/10.1007/s12666-014-0429-0.
[24] A. Maurotto, C.T. Wickramarachchi, Experimental investigations on effects of frequency in ultrasonically-assisted end-milling of AISI 316L: a feasibility study, Ultrasonics 65 (2016) 113–120, https://doi.org/10.1016/j.ultras.2015.10.012.
[25] S. Elhami, M.R. Razfar, M. Farahnakian, Analytical, numerical and experimental study of cutting force during thermally enhanced ultrasonic assisted milling of hardened AISI 4140, Int. J. Mech. Sci. 103 (2015) 158–171, https://doi.org/10.1016/j.ijmecsci.2015.09.007.
[26] M.R. Razfar, P. Sarvi, M.M.A. Zarchi, Experimental investigation of the surface roughness in ultrasonic-assisted milling, Proc. Inst. Mech. Eng. Part B J. Eng. Manuf. 225 (2011) 1615–1620, https://doi.org/10.1177/0954405411399331.
[27] K. Marcel, Z. Marek, P. Jozef, Investigation of ultrasonic assisted milling of aluminum alloy AlMg4.5Mn, Proc. Eng. 69 (2014) 1048–1053, https://doi.org/10.1016/j.proeng.2014.03.089.
[28] N.F.H.A. Halim, H. Ascroft, S. Barnes, Analysis of tool wear, cutting force, surface roughness and machining temperature during finishing operation of ultrasonic assisted milling (UAM) of carbon fibre reinforced plastic (CFRP), Proc. Eng. 184 (2017) 185–191, https://doi.org/10.1016/j.proeng.2017.04.084.
[29] Y. Wang, H. Gong, F.Z. Fang, H. Ni, Kinematic view of the cutting mechanism of rotary ultrasonic machining by using spiral cutting tools, Int. J. Adv. Manuf. Technol. 83 (2016) 461–474, https://doi.org/10.1007/s00170-015-7549-5.
[30] G.C. Verma, P.M. Pandey, U.S. Dixit, Modeling of static machining force in axial ultrasonic-vibration assisted milling considering acoustic softening, Int. J. Mech. Sci. 136 (2018) 1–16, https://doi.org/10.1016/j.ijmecsci.2017.11.048.
[31] A.R. Machado, J. Wallbank, The effect of extremely low lubricant volumes in machining, Wear 210 (1997) 76–82, https://doi.org/10.1016/S0043-1648(97)00059-8.
[32] P. Lee, Y. Altintaş, Prediction of ball-end milling forces from orthogonal cutting data, Int. J. Mach. Tools Manuf. 36 (1996) 1059–1072, https://doi.org/10.1016/0890-6955(95)00081-X.
[33] R. Myres, D. Montgomery, C. Anderson, Process and Product Optimization Using Designed Experiments, John Wiley Sons, New York, 2009, pp. 1–25.
[34] C.C. Bissell, Nyquist rate sampling, Int. J. Electr. Eng. Educ. 27 (1990) 77–79, https://doi.org/10.1177/002072099002700116.
[35] S.Y. Liangt, J.J.J. Wang, Milling forces convolution modeling for identification of cutter axis offset, Int. J. Mach. Tools Manuf. 34 (1994) 1177–1190.
[36] H. Li, X. Li, Modelling and simulation of chatter in milling using a predictive force model, Int. J. Mach. Tools Manuf. 40 (2000) 2047–2071, https://doi.org/10.1016/S0890-6955(00)00042-0.
[37] W.F. Hastings, P. Mathew, P.L.B. Oxley, A machining theory for predicting chip geometry, cutting forces etc. from work material properties and cutting conditions, Proc. R. Soc. A Math. Phys. Eng. Sci. 371 (1980) 569–587, https://doi.org/10.1098/rspa.1980.0097.
[38] A. Siddiq, T. El Sayed, Ultrasonic-assisted manufacturing processes: variational model and numerical simulations, Ultrasonics 52 (2012) 521–529, https://doi.org/10.1016/j.ultras.2011.11.004.
[39] Z. Yao, G.Y. Kim, Z. Wang, L. Faidley, Q. Zou, D. Mei, Z. Chen, Acoustic softening and residual hardening in aluminum: modeling and experiments, Int. J. Plast. 39 (2012) 75–87, https://doi.org/10.1016/j.ijplas.2012.06.003.
[40] E. Budak, Y. Altintaş, E.J.A. Armarego, Prediction of milling force coefficients from orthogonal cutting data, J. Manuf. Sci. Eng. 118 (1996) 216, https://doi.org/10.1115/1.2831014.
[41] S. Kuriakose, M.S. Shunmugam, Multi-objective optimization of wire-electro discharge machining process by non-dominated sorting genetic algorithm, J. Mater. Process. Technol. 170 (2005) 133–141, https://doi.org/10.1016/j.jmatprotec.2005.04.105.